Image Reconstruction 2: Compressed Sensing & Low-Rank Models

Zhengguo Tan, Ph.D.

Michigan Institute for Imaging Technology and Translation (MIITT)
University of Michigan, Ann Arbor, Michigan, USA

September 30, 2025

Outline

Funny Intro to Compressed Sensing

Compressed Sensing: Definition

Stable Signal Recovery from
Incomplete and Inaccurate Measurements

Emmanuel Candes[†], Justin Romberg[†], and Terence Tao[♯]

† Applied and Computational Mathematics, Caltech, Pasadena, CA 91125

♯ Department of Mathematics, University of California, Los Angeles, CA 90095

February, 2005; Revised June, 2005

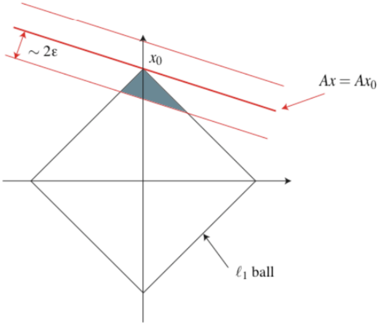

$$\min \|x\|_{\ell_1} \quad \text{subject to } \|Ax - y\|_{\ell_2} \leq \epsilon \qquad (1)$$

$$\operatorname*{argmin}_x \|Ax - y\|_2 + \lambda \|Rx\|_1 \qquad (2)$$

Compressed Sensing MRI

Magnetic Resonance in Medicine 58:1182–1195 (2007)

Sparse MRI: The Application of Compressed Sensing for Rapid MR Imaging

Michael Lustig,[1*] David Donoho,[2] and John M. Pauly[1]

Compressed Sensing: Funny Intro from Miki Lustig

Source: https://people.eecs.berkeley.edu/~mlustig/comics0.html

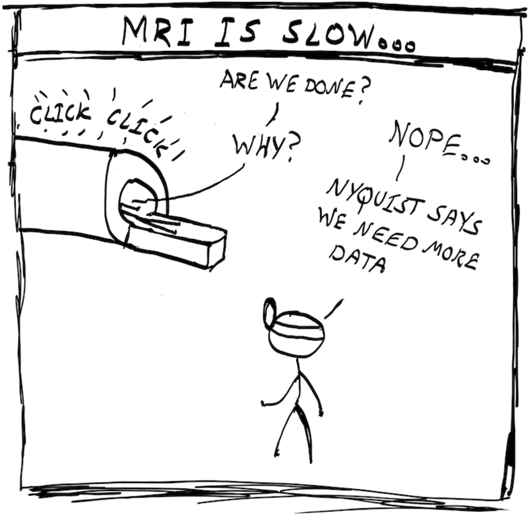

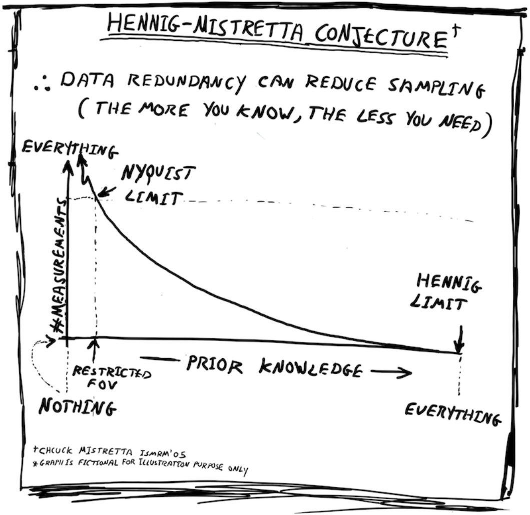

Compressed Sensing: Funny Intro from Miki Lustig

Source: https://people.eecs.berkeley.edu/~mlustig/comics0.html

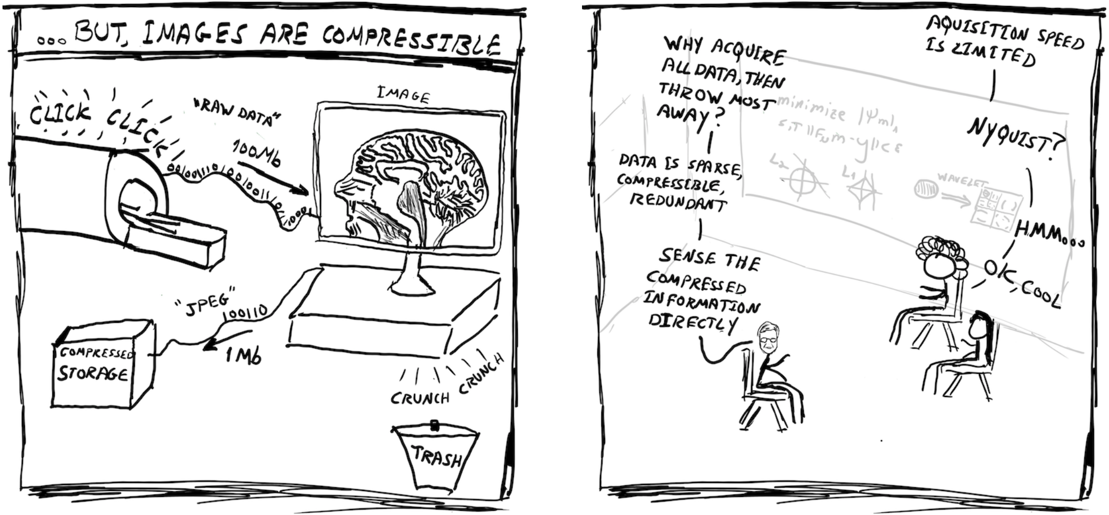

Compressed Sensing: Funny Intro from Miki Lustig

Source: https://people.eecs.berkeley.edu/~mlustig/comics0.html

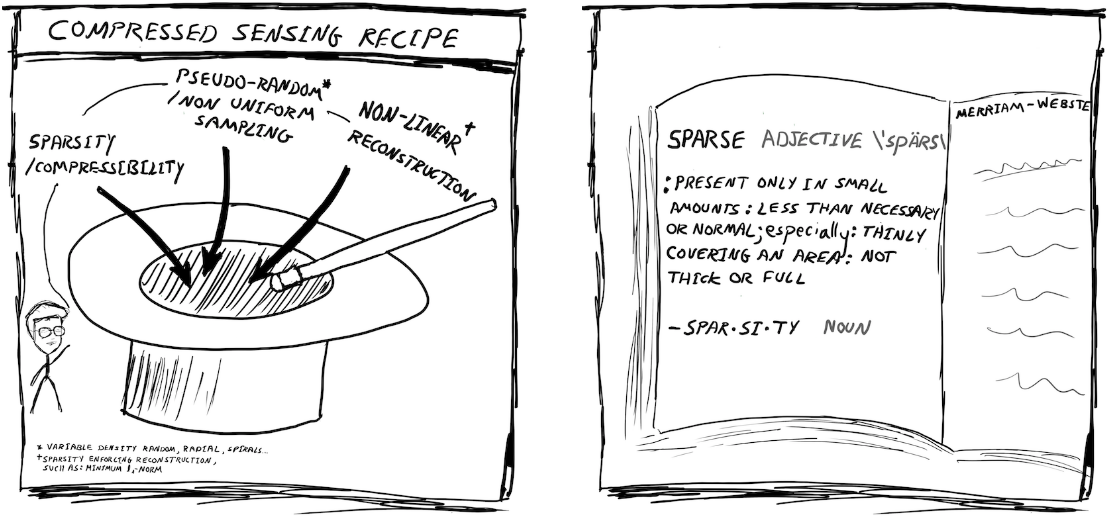

Compressed Sensing: Funny Intro from Miki Lustig

Source: https://people.eecs.berkeley.edu/~mlustig/comics0.html

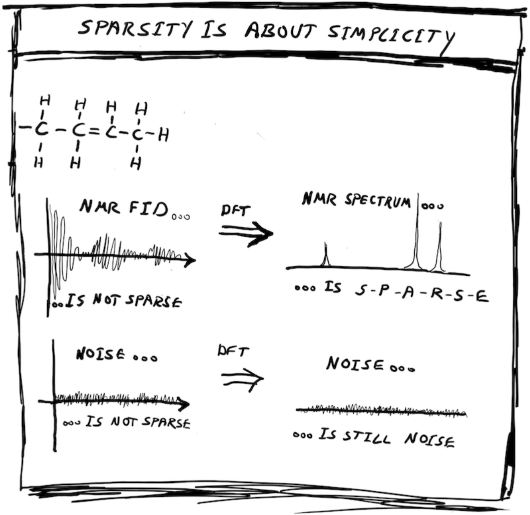

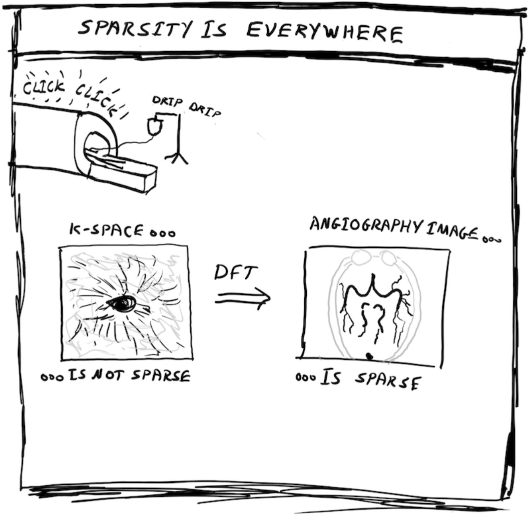

Compressed Sensing: Funny Intro from Miki Lustig

Source: https://people.eecs.berkeley.edu/~mlustig/comics0.html

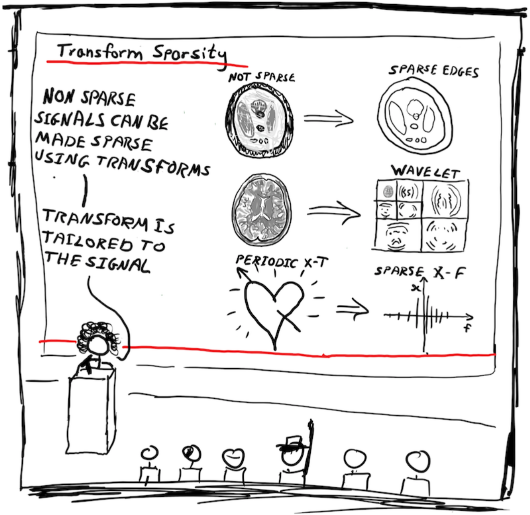

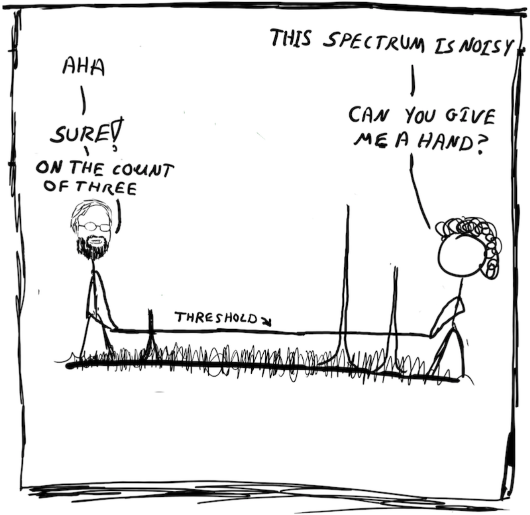

Compressed Sensing: Funny Intro from Miki Lustig

Source: https://people.eecs.berkeley.edu/~mlustig/comics0.html

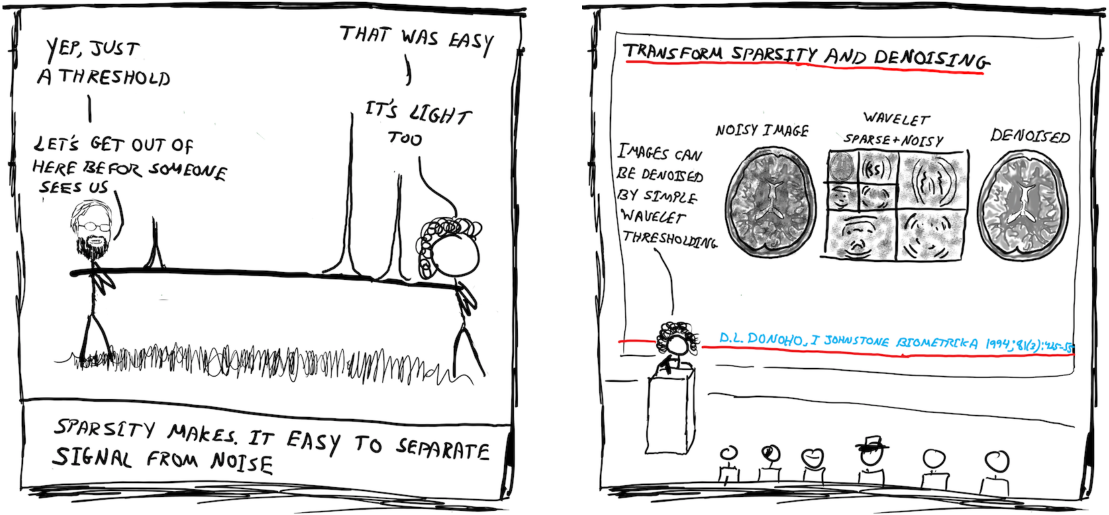

Compressed Sensing: Funny Intro from Miki Lustig

Source: https://people.eecs.berkeley.edu/~mlustig/comics0.html

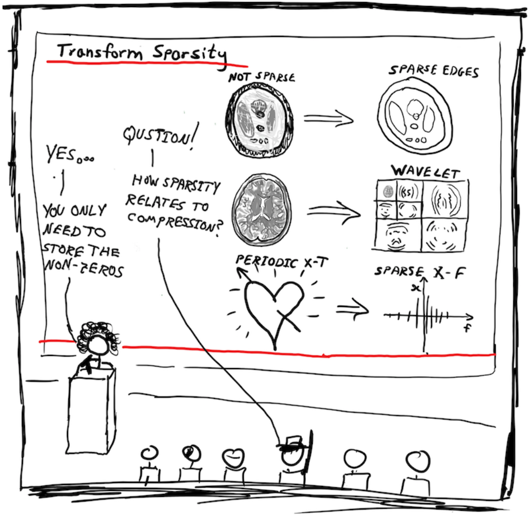

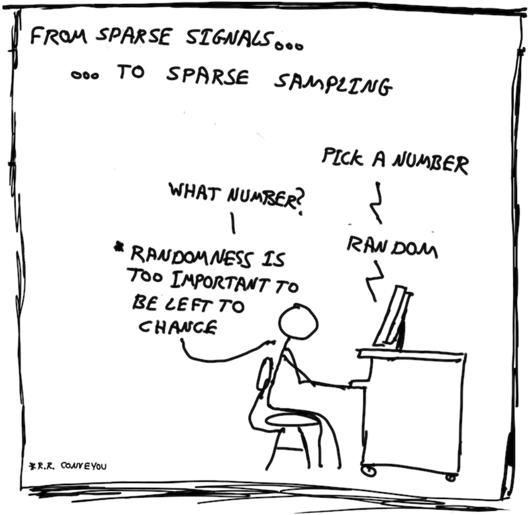

Compressed Sensing: Funny Intro from Miki Lustig

Source: https://people.eecs.berkeley.edu/~mlustig/comics0.html

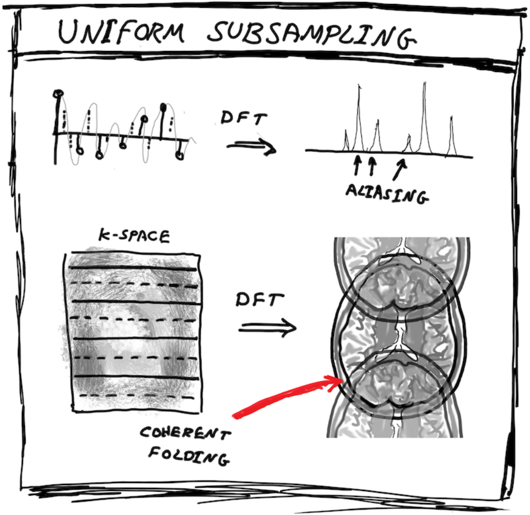

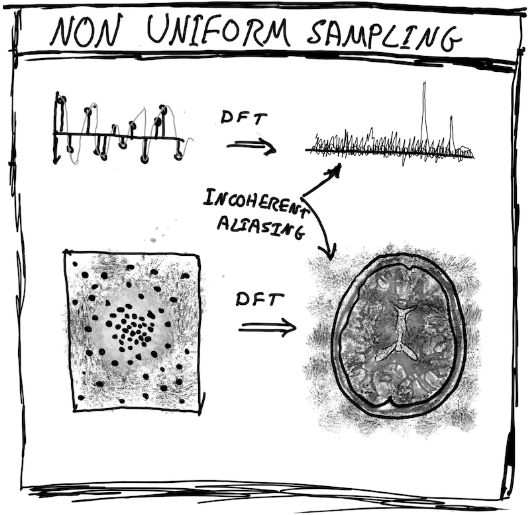

Compressed Sensing: Funny Intro from Miki Lustig

Source: https://people.eecs.berkeley.edu/~mlustig/comics0.html

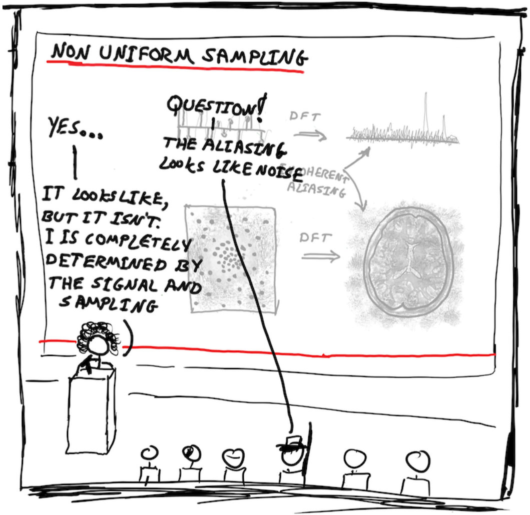

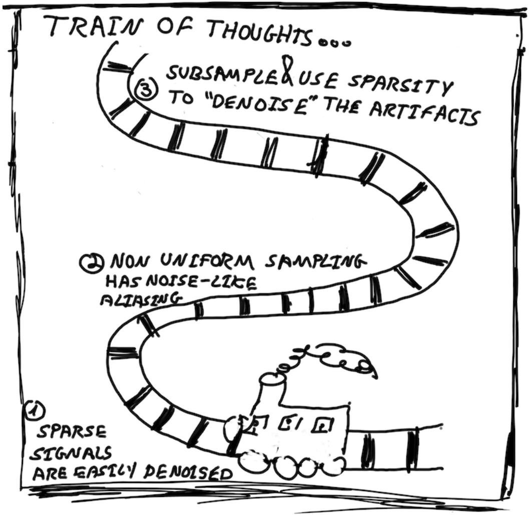

Compressed Sensing: Funny Intro from Miki Lustig

Source: https://people.eecs.berkeley.edu/~mlustig/comics0.html

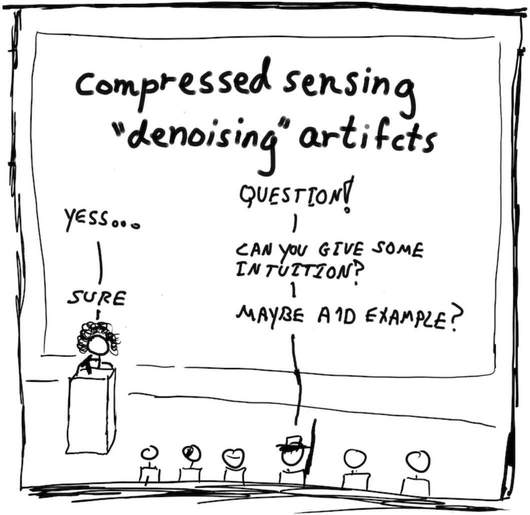

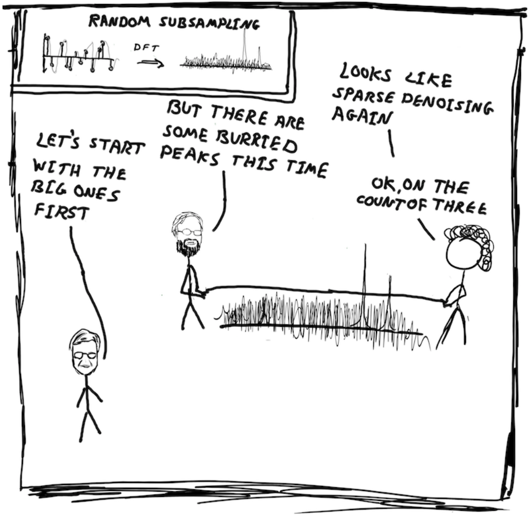

Compressed Sensing: Funny Intro from Miki Lustig

Source: https://people.eecs.berkeley.edu/~mlustig/comics0.html

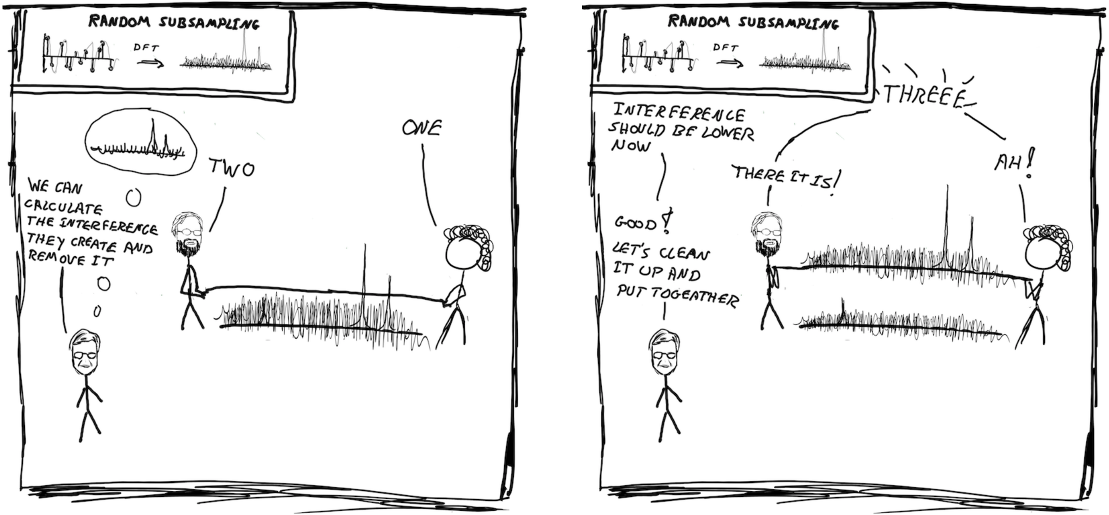

Compressed Sensing: Funny Intro from Miki Lustig

Source: https://people.eecs.berkeley.edu/~mlustig/comics0.html

Compressed Sensing

Ingredients in Compressed Sensing

1. Sparsity
2. Incoherence: Non-uniform sampling
3. Non-linear reconstruction

Examples of Sparsity Transform: Wavelet & Total Variation

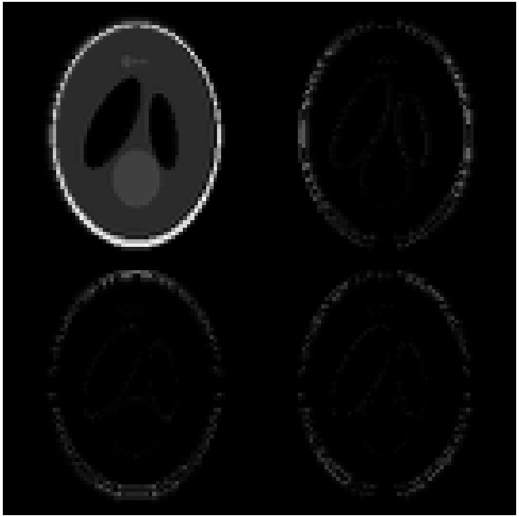

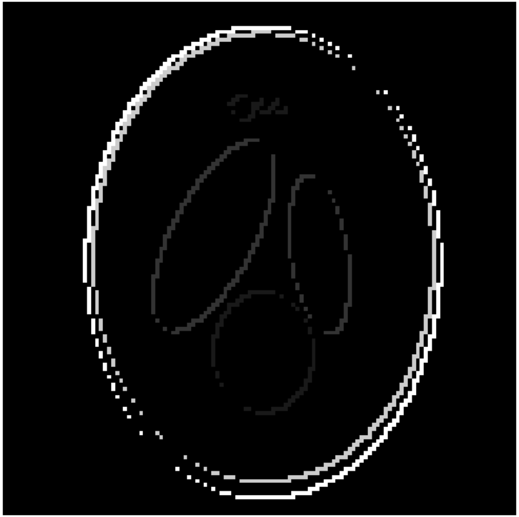

Uniform Undersampling

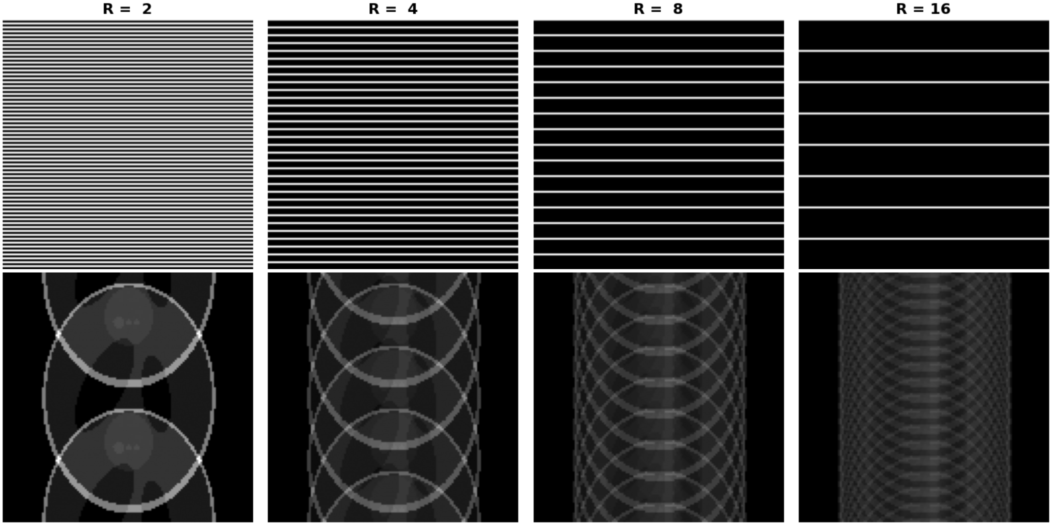

Non-Uniform Undersampling: Poisson

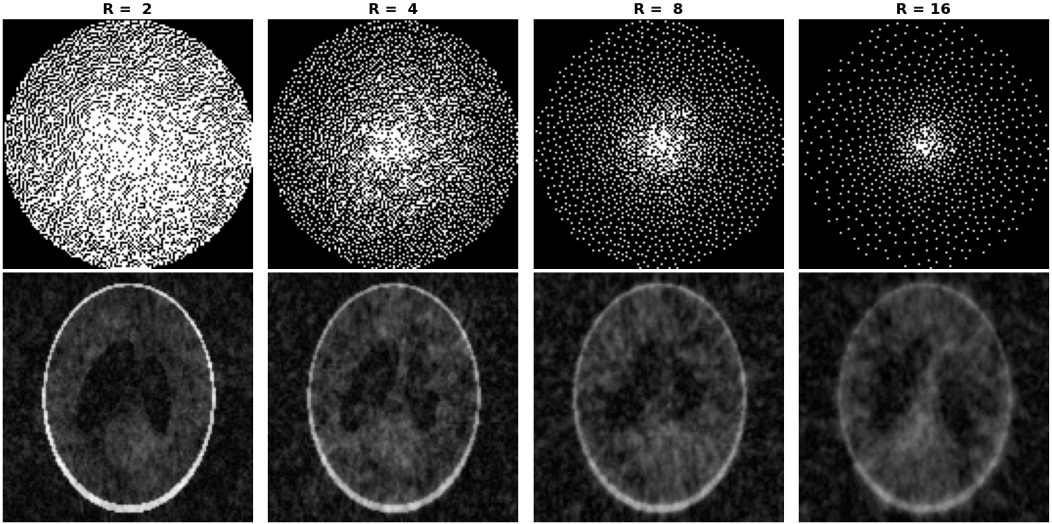

Non-Uniform Undersampling: Radial

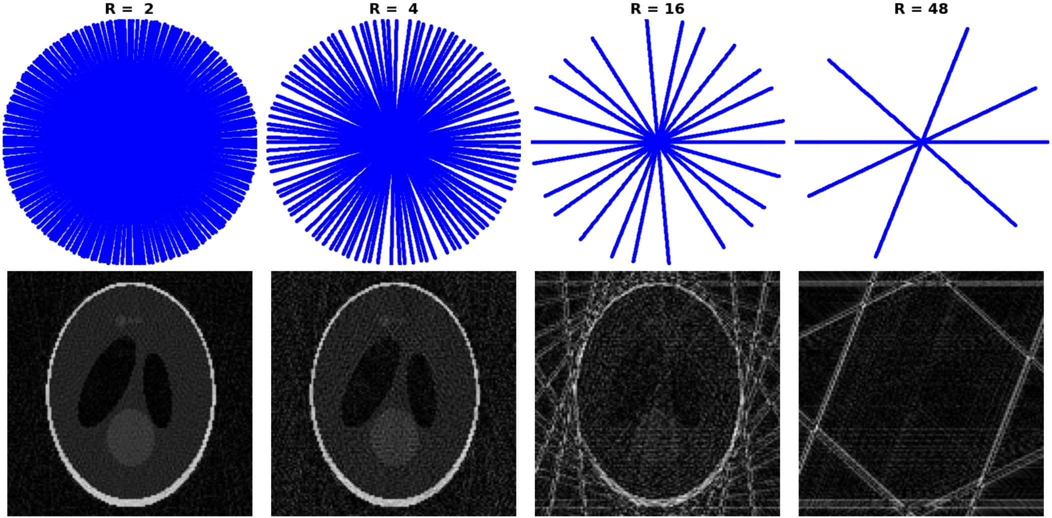

Non-Uniform Undersampling: Spiral

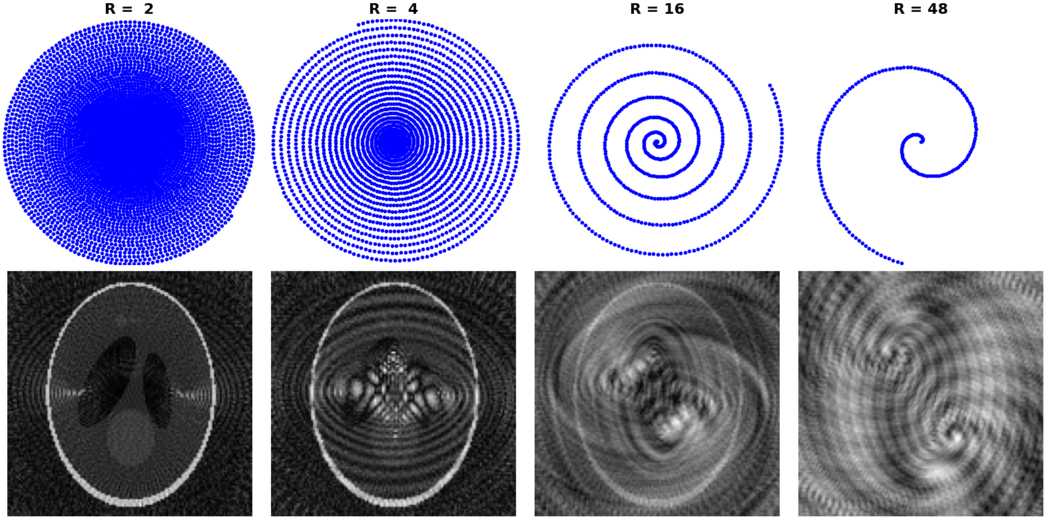

Understand Incoherence via Point Spread Function (PSF)

- the response of a focused optical imaging system to a point source or point object
- the impulse response function of a focused optical imaging system

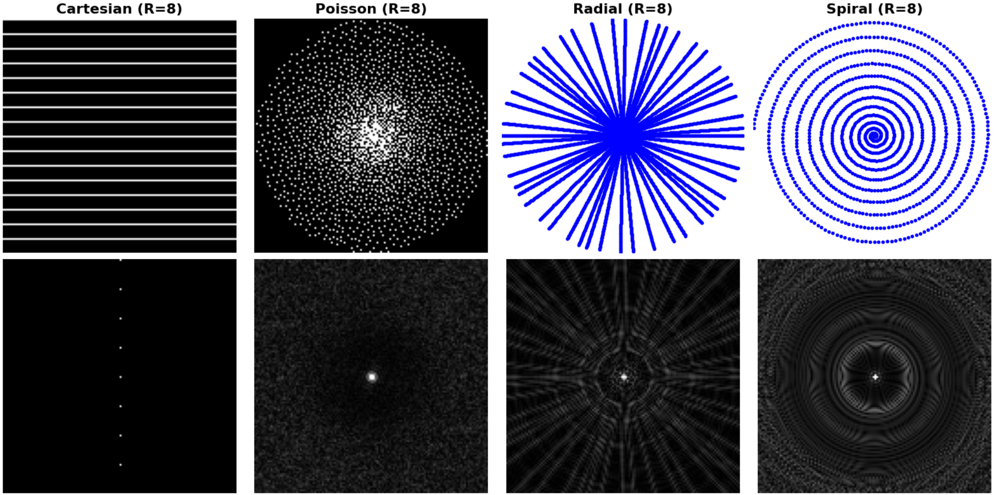

Non-Linear Reconstruction

1. ℓ_1 regularization with soft thresholding for linear inverse problem
   - Beck A, Teboulle M. A fast iterative shrinkage-thresholding algorithm for linear inverse problems. *SIAM J Imaging Sciences* (2009).

2. Non-linear model-based reconstruction
   - Block KT, Uecker M, Frahm J. Model-based iterative reconstruction for radial fast spin-echo MRI. *IEEE Trans Med Imaging* (2009).
   - Fessler JA. Model-based image reconstruction for MRI. *IEEE Signal Process Mag* (2010).
   - Doneva M, Börnert P, Eggers H, Stehning C, Sénégas J, Mertins A. Compressed sensing reconstruction for magnetic resonance parameter mapping. *Magn Reson Med* (2010).
   - Ma D, Gulani V, Seiberlich N, et al. Magnetic resonance fingerprinting. *Nature* (2013).

Let's Begin with Parallel Imaging as Linear Inverse Problem

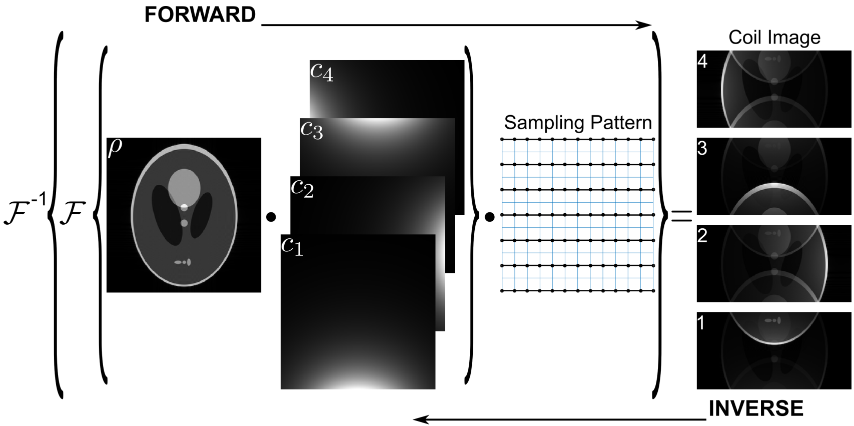

$$\underset{x}{\operatorname{argmin}} \|y - \mathbf{PFC}x\|_2 + \lambda \|x\|_2 \qquad (3)$$

Solution

- Gradient update rule:

$$x^{(k+1)} = x^{(k)} - \alpha \mathbf{C}^* \mathbf{F}^{-1} \mathbf{P}^* (y - \mathbf{PFC} x^{(k)}) \tag{4}$$

- Can be solved efficiently by gradient descent, conjugate gradient, ...

Sparsity Constraint

$$\underset{x}{\operatorname{argmin}} \|y - \mathbf{PFC}x\|_2 + \lambda \|\mathbf{R}x\|_1 \tag{5}$$

- ℓ_1 function is not differentiable

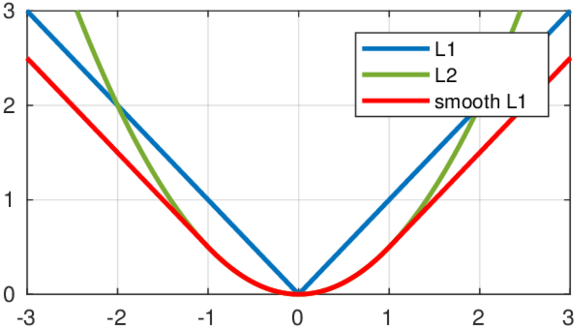

Feng ZH, Kittler J, Awais M, Huber P. Wing loss for robust facial landmark localisation with CNN. *CVPR* (2018).

Fast Iterative Soft Thresholding (FISTA)

FISTA with constant stepsize

Input: $L = L(f)$ - A Lipschitz constant of ∇f.

Step 0. Take $\mathbf{y}_1 = \mathbf{x}_0 \in \mathbb{R}^n$, $t_1 = 1$.

Step k. $(k \geq 1)$ Compute

$$\mathbf{x}_k = p_L(\mathbf{y}_k), \tag{4.1}$$

$$t_{k+1} = \frac{1 + \sqrt{1 + 4t_k^2}}{2}, \tag{4.2}$$

$$\mathbf{y}_{k+1} = \mathbf{x}_k + \left(\frac{t_k - 1}{t_{k+1}}\right)(\mathbf{x}_k - \mathbf{x}_{k-1}). \tag{4.3}$$

- the function p is defined as:

$$x^{(k+1)} = \mathcal{T}_{\lambda\alpha}(x^{(k)} - \alpha \mathbf{A}^T(\mathbf{A}x^{(k)} - b)) \tag{6}$$

$$\mathcal{T}_c = (|x| - c)_+ \mathrm{sgn}(x) \tag{7}$$

Toy Example

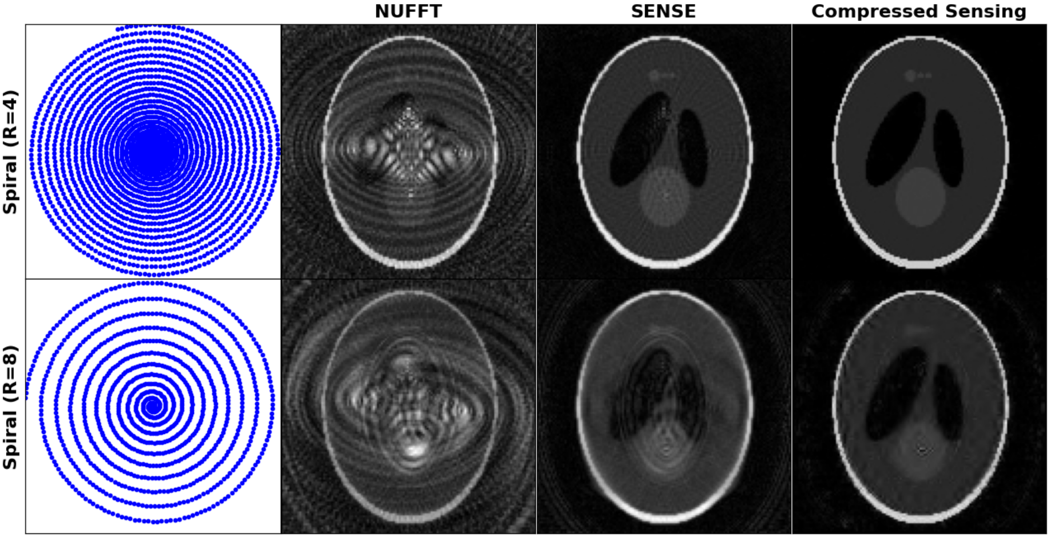

Beyond 2D: k-t Sparsity [1]

representation. We demonstrate a 7-fold frame-rate acceleration both in simulated data and *in vivo* non-gated Cartesian balanced-SSFP cardiac MRI .

Theory

Dynamic MR images are highly redundant in space and time. By using linear transformations (such as wavelets, Fourier etc.), we can represent a dynamic scene using only a few sparse transform coefficients. Inadequate sampling of the spatial-frequency -- temporal space (k-t space) results in aliasing in the spatial -- temporal-frequency space (x-f space). The aliasing artifacts due to random under-sampling are incoherent as opposed to coherent artifacts in equispaced under sampling. More importantly the artifacts are incoherent in the sparse transform domain. By using the non-linear reconstruction scheme in [1-5] we can recover the sparse transform coefficients and as a consequence, recover the dynamic scene. We exploit sparsity by constraining our reconstruction to have a sparse representation and be consistent with the measured data by solving the constrained optimization problem: *minimize* $\|\Psi m\|_1$ *subject to:* $\|Fm - y\|_2 < \varepsilon$. Here m is the dynamic scene, Ψ transforms the scene into a sparse representation, F is randomized phase encode ordering Fourier matrix, y is the measured k-space data and ε controls fidelity of the reconstruction to the measured data. ε is usually set to the noise level.

Methods

For dynamic heart imaging, we propose using the wavelet transform in the spatial dimension and the Fourier transform in the temporal. Wavelets sparsify

reconstruction.

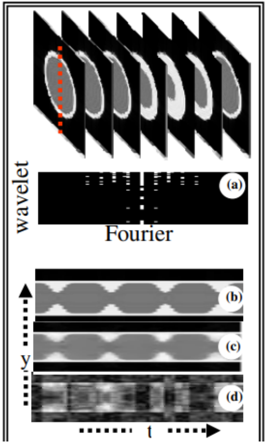

Figure 2: *Simulated dynamic data. (a) The transform domain of the cross section is truly sparse. (b) Ground truth cross-section. (c) L_1 reconstruction from random phase encode ordering, 4-fold acceleration (d) Sliding window (64) reconstruction from random phase encode ordering..*

Figure 3:*Dynamic SSFP heart imaging with randomized ordering. 7 - fold acceleration (25FPS). The images show two frames of the heart phase and a cross section evolution in time (a) Sliding window (64) recon. (b) L_1 recon. The signal is recovered in both time and space using the L_1 method.*

[1] Lustig M, Santos JM, Donoho DL, Pauly JM. k-t SPARSE: High frame rate dynamic MRI exploiting spatio-temporal sparsity. *ISMRM* (2006).

Non-Linear Model-Based Reconstruction

- From parallel imaging to high-dimensional imaging

Non-Linear Model-Based Reconstruction

- From parallel imaging to high-dimensional imaging
- Can we chain the Bloch equation into the parallel imaging forward model?

$$\underset{x}{\operatorname{argmin}} \|y - \mathbf{PFCB}x\|_2 + \lambda \mathbf{R}(x) \tag{8}$$

Non-Linear Model-Based Reconstruction

- From parallel imaging to high-dimensional imaging
- Can we <u>chain</u> the Bloch equation into the parallel imaging forward model?

$$\underset{x}{\operatorname{argmin}} \|y - \mathbf{PFCB}x\|_2 + \lambda \mathbf{R}(x) \tag{8}$$

- Examples of **B**:

$$\mathbf{B}(M_0, T_2) := M_0 \cdot e^{-t/T_2} \tag{9}$$

$$\mathbf{B}(M_{ss}, M_0, T_1) := M_{ss} - (M_{ss} + M_0) \cdot e^{-t/T_1^*} \tag{10}$$

$$\mathbf{B}(\mathrm{W}, \mathrm{F}, T_2^*, f_{B_0}) := (\mathrm{W} + \mathrm{F} \cdot z_t) \cdot e^{-i2\pi f_{B_0} t} \cdot e^{-t/T_2^*} \tag{11}$$

$$\cdots \tag{12}$$

Example: Phase-Contrast Flow

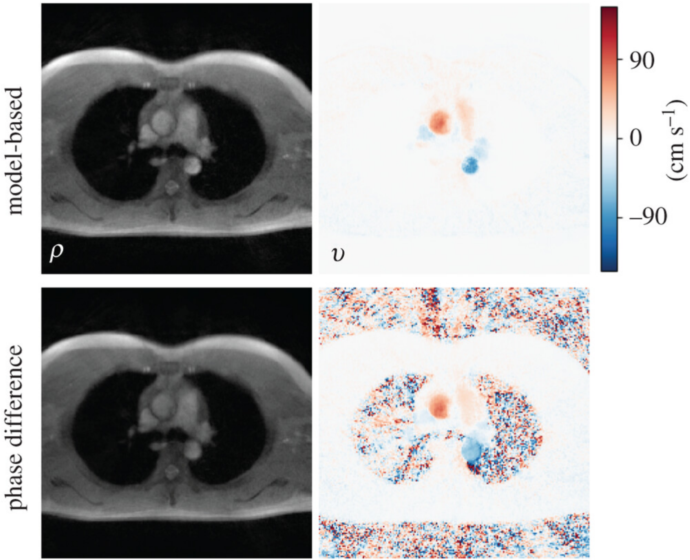

Example: Fat, T_2^*, and B_0 Field Inhomogeneity

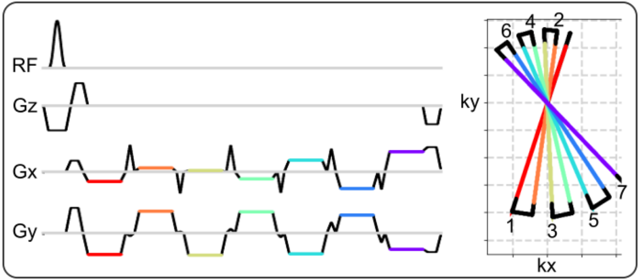

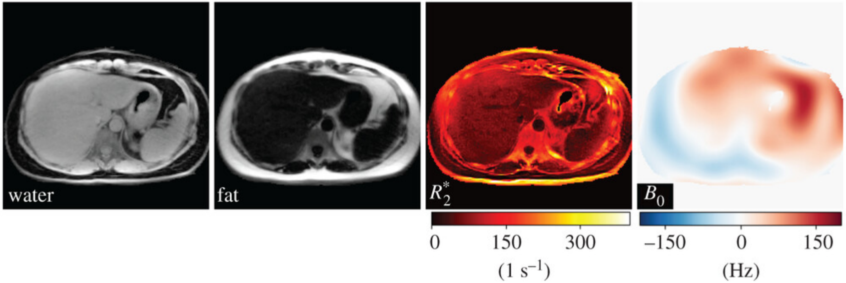

Low Rank

Matrix Rank [2]

- In linear algebra, the rank of a matrix is the dimension of the vector space spanned by its columns.

$$\begin{bmatrix} 1 & 2 & 1 \\ -2 & -3 & 1 \\ 3 & 5 & 0 \end{bmatrix} \xrightarrow{2R_1+R_2\to R_2} \begin{bmatrix} 1 & 2 & 1 \\ 0 & 1 & 3 \\ 3 & 5 & 0 \end{bmatrix} \xrightarrow{-3R_1+R_3\to R_3} \begin{bmatrix} 1 & 2 & 1 \\ 0 & 1 & 3 \\ 0 & -1 & -3 \end{bmatrix}$$
$$\xrightarrow{R_2+R_3\to R_3} \begin{bmatrix} 1 & 2 & 1 \\ 0 & 1 & 3 \\ 0 & 0 & 0 \end{bmatrix} \xrightarrow{-2R_2+R_1\to R_1} \begin{bmatrix} 1 & 0 & -5 \\ 0 & 1 & 3 \\ 0 & 0 & 0 \end{bmatrix}.$$

The final matrix (in reduced row echelon form) has two non-zero rows and thus the rank of matrix A is 2.

[2] https://en.wikipedia.org/wiki/Rank_(linear_algebra)

Matrix Rank [2]

- In linear algebra, the rank of a matrix is the dimension of the vector space spanned by its columns.

$$\begin{bmatrix} 1 & 2 & 1 \\ -2 & -3 & 1 \\ 3 & 5 & 0 \end{bmatrix} \xrightarrow{2R_1+R_2 \to R_2} \begin{bmatrix} 1 & 2 & 1 \\ 0 & 1 & 3 \\ 3 & 5 & 0 \end{bmatrix} \xrightarrow{-3R_1+R_3 \to R_3} \begin{bmatrix} 1 & 2 & 1 \\ 0 & 1 & 3 \\ 0 & -1 & -3 \end{bmatrix}$$
$$\xrightarrow{R_2+R_3 \to R_3} \begin{bmatrix} 1 & 2 & 1 \\ 0 & 1 & 3 \\ 0 & 0 & 0 \end{bmatrix} \xrightarrow{-2R_2+R_1 \to R_1} \begin{bmatrix} 1 & 0 & -5 \\ 0 & 1 & 3 \\ 0 & 0 & 0 \end{bmatrix}.$$

The final matrix (in reduced row echelon form) has two non-zero rows and thus the rank of matrix A is 2.

- Matrix rank can be computed via singular value decomposition (SVD).

[2] https://en.wikipedia.org/wiki/Rank_(linear_algebra)

SPATIOTEMPORAL IMAGING WITH PARTIALLY SEPARABLE FUNCTIONS

Zhi-Pei Liang

Department of Electrical and Computer Engineering, and
Beckman Institute for Advanced Science and Technology
University of Illinois at Urbana-Champaign

Spatio-Temporal Imaging

2.2. Spatiotemporal Model using PSF

We propose to use (4) to model $\rho(\mathbf{r},t)$ by assuming that spatial variations are separable from temporal variations to the Lth-order. Equivalently, $s(\mathbf{k},t)$ is Lth-order partially separable in the following sense

$$s(\mathbf{k},t) = \sum_{\ell=1}^{L} c_\ell(\mathbf{k})\varphi_\ell(t) \tag{5}$$

The following theorem provides the necessary and sufficient conditions for (5).

Theorem 2.4. *Assume that $s(\mathbf{k},t)$ is defined over $\mathcal{K}\times\mathcal{T}$ with $\mathcal{K} = \{\mathbf{k}_1, \mathbf{k}_2, \ldots, \mathbf{k}_n\}$ and $\mathcal{T} = \{t_1, t_2, \ldots, t_m\}$. Let*

$$\mathbf{C} = \begin{bmatrix} s(\mathbf{k}_1,t_1) & s(\mathbf{k}_1,t_2) & \cdots & s(\mathbf{k}_1,t_m) \\ s(\mathbf{k}_2,t_1) & s(\mathbf{k}_2,t_2) & \cdots & s(\mathbf{k}_2,t_m) \\ \vdots & & \ddots & \vdots \\ s(\mathbf{k}_n,t_1) & s(\mathbf{k}_n,t_2) & \cdots & s(\mathbf{k}_n,t_m) \end{bmatrix} \tag{6}$$

(5) is exact if and only if $\mathbf{C}$ is rank L with $L < \min\{m,n\}$.

In practice, $s(\mathbf{k},t)$ is corrupted by noise. Determination of the *effective* rank of $\mathbf{C}$ will be discussed in the *image reconstruction* section.

The PSF model in (5) can also be justified heuristically. Equivalent to (5), we have

$$\rho(\mathbf{r},t) = \sum_{\ell=1}^{L} \tilde{c}_\ell(\mathbf{r})\varphi_\ell(t) \tag{7}$$

Toy Example

dynamic image seris

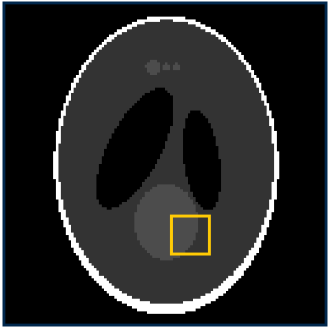

spatio-temporal matrix

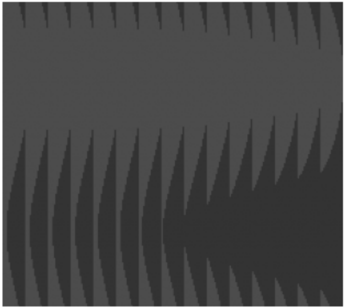

eigenvalues

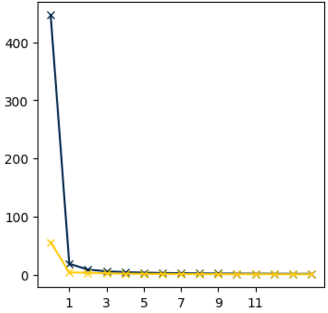

Locally Low Rank [3]

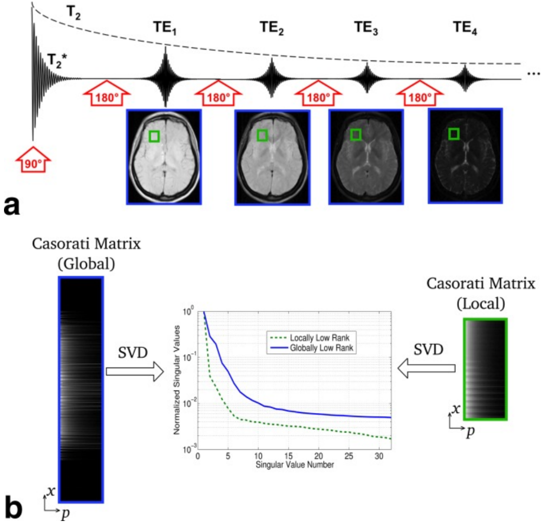

[3] Zhang T, Pauly JM, Levesque IR. Accelerating parameter mapping with a locally low rank constraint. *Magn Reson Med* (2015).

Low Rank Approximation of Bloch Models [4,5]

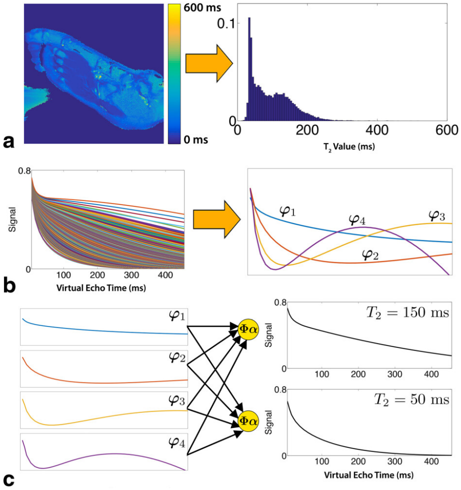

- define echo images with the shape $[N_x, N_y, N_t]$

$$\rho_t = M_0 \cdot e^{-t/T_2} \tag{13}$$

[4] Huang C, Graff CG, Clarkson EW, Bilgin A, Altbach MI. T_2 mapping from highly undersampled data by reconstruction of principle component coefficient maps using compressed sensing. *Magn Reson Med* (2012).

[5] Tamir JI, Uecker M, Chen W, et al. T_2 shuffling: sharp, multicontrast, volumetric fast spin-echo imaging. *Magn Reson Med* (2017).

Low Rank Approximation of Bloch Models [4,5]

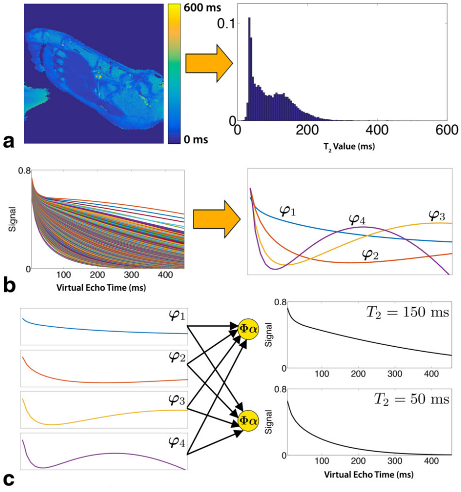

- define echo images with the shape $[N_x, N_y, N_t]$

$$\rho_t = M_0 \cdot e^{-t/T_2} \tag{13}$$

- With low rank approximation

$$\rho = \Phi\alpha \tag{14}$$

$$\Phi : [N_t, K] \tag{15}$$

$$\alpha : [N_x, N_y, K] \tag{16}$$

[4] Huang C, Graff CG, Clarkson EW, Bilgin A, Altbach MI. T_2 mapping from highly undersampled data by reconstruction of principle component coefficient maps using compressed sensing. *Magn Reson Med* (2012).

[5] Tamir JI, Uecker M, Chen W, et al. T_2 shuffling: sharp, multicontrast, volumetric fast spin-echo imaging. *Magn Reson Med* (2017).

Low Rank Approximation of Bloch Models [4,5]

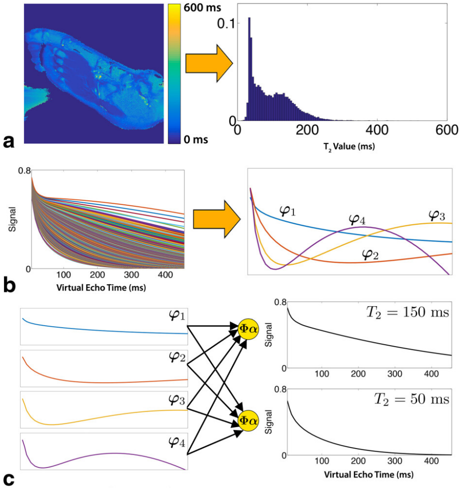

- define echo images with the shape $[N_x, N_y, N_t]$

$$\rho_t = M_0 \cdot e^{-t/T_2} \tag{13}$$

- With low rank approximation

$$\rho = \Phi\alpha \tag{14}$$

$$\Phi : [N_t, K] \tag{15}$$

$$\alpha : [N_x, N_y, K] \tag{16}$$

- $K << N_t$ AND It's a linear model!

[4] Huang C, Graff CG, Clarkson EW, Bilgin A, Altbach MI. T_2 mapping from highly undersampled data by reconstruction of principle component coefficient maps using compressed sensing. *Magn Reson Med* (2012).

[5] Tamir JI, Uecker M, Chen W, et al. T_2 shuffling: sharp, multicontrast, volumetric fast spin-echo imaging. *Magn Reson Med* (2017).

Low Rank Image Reconstruction

$$\underset{x}{\operatorname{argmin}} \|y - \mathbf{PFC\Phi}x\|_2 + \lambda \mathbf{R}(x) \tag{17}$$

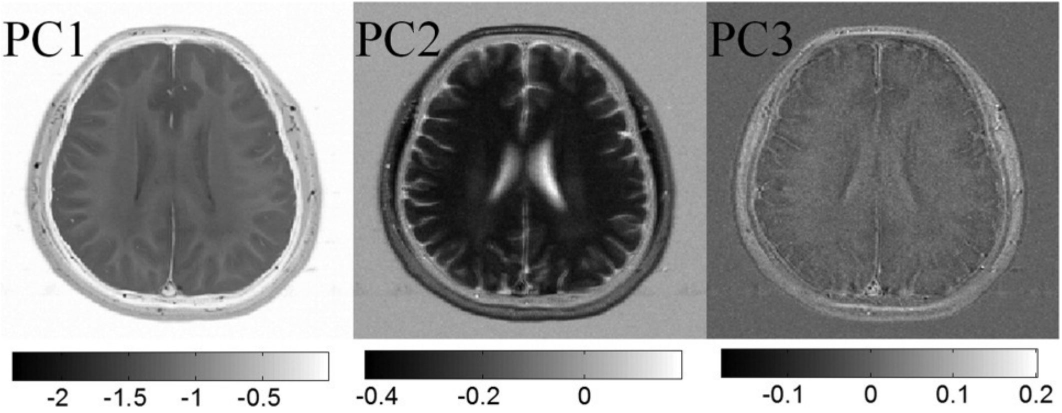

Low Rank for Magnetic Resonance Fingerprinting (MRF) [6]

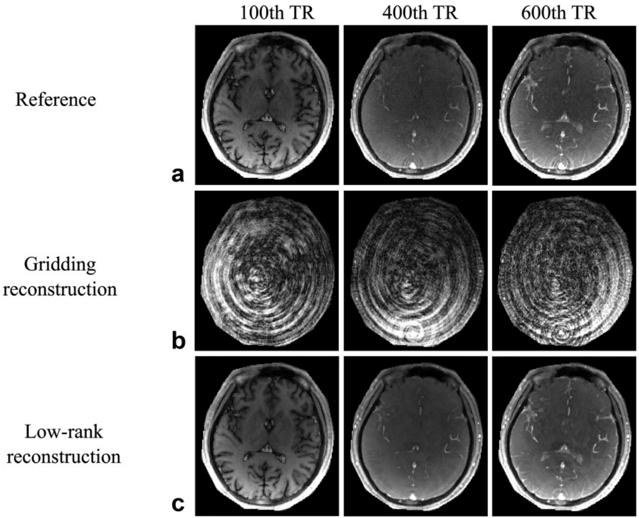

[6] Zhao B, Setsompop K, Adalsteinsson E, et al. Improved MRF reconstruction with low-rank and subspace modeling. *Magn Reson Med* (2018).

Structured Low Rank

- Mapping image series into structured matrices (e.g., Toeplitz or Hankel) to restore the complete image series
- MR examples:
  1. ESPIRiT: coil calibration; where SENSE meets GRAPPA;
  2. MUSSELS: multi-shot diffusion MRI reconstruciton.

ESPIRiT: An eigenvalue approach to autocalibrating parallel MRI

- Walsh DO, Gmitro AF, Marcellin MW. Adaptive reconstruction of phased array MR imagery. *Magn Reson Med* (2000).
- Zhang J, Liu C, Moseley ME. Parallel reconstruction using null operations. *Magn Reson Med* (2011).
- Lai P, Lustig M, Brau AC, Vasanawala S, Beatty PJ, Alley M. Efficient L1SPIRiT reconstruction (ESPIRiT) for highly accelerated 3D volumetric MRI with parallel imaging and compressed sensing. *ISMRM* (2010).
- Lustig M, Lai P, Murphy M, Vasanawala SS, Elad M, Zhang J, Pauly JM. An eigen-vector approach to autocalibrating parallel MRI, where SENSE meets GRAPPA. *ISMRM* (2011).
- Uecker M, Lai P, Murphy MJ, et al. ESPIRiT - an eigenvalue approach to autocalibrating parallel MRI: where SENSE meets GRAPPA. *Magn Reson Med* (2014).

ESPIRiT

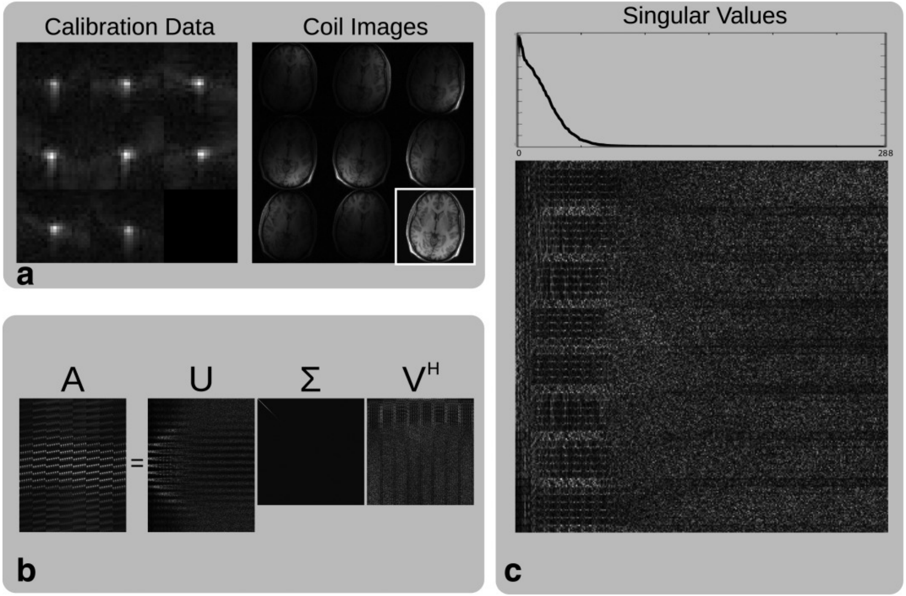

Calibration Data
Coil Images
a
A
=
U
Σ
V^H
b
Singular Values
0
288
c

ESPIRiT

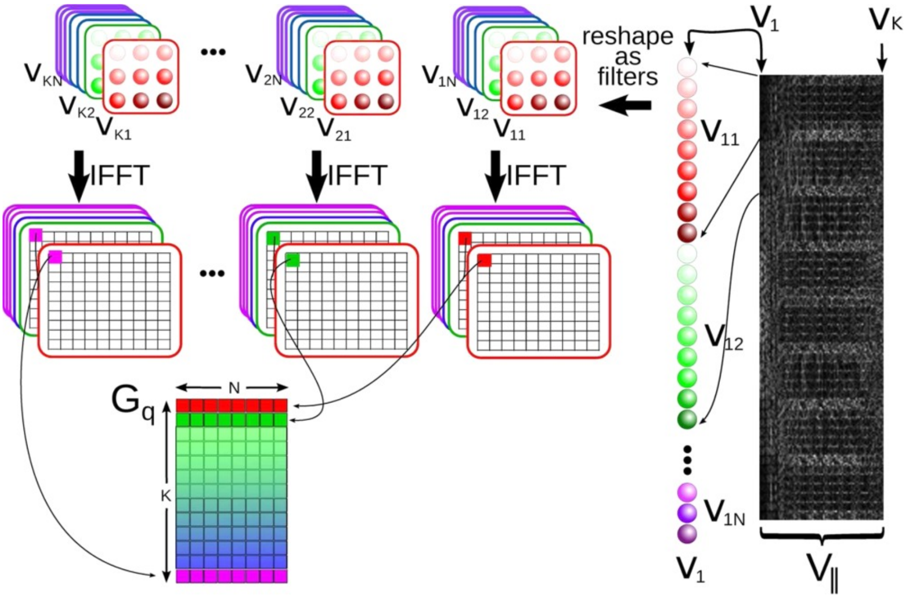

V_{KN}
V_{K2}
V_{K1}
V_{2N}
V_{22}
V_{21}
V_{1N}
V_{12}
V_{11}
reshape as filters
V_1
V_K
IFFT
IFFT
IFFT
V_{11}
V_{12}
V_{1N}
V_1
$V_{\|}$
G_q
N
K

ESPIRiT

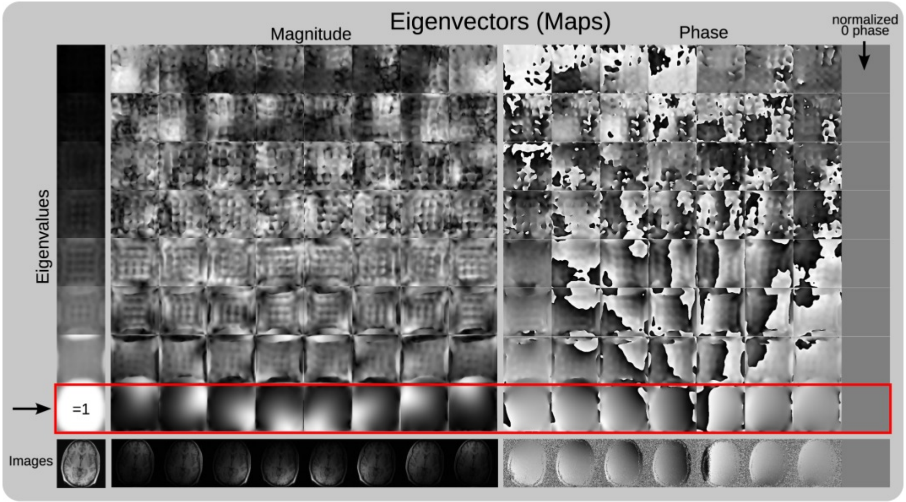

Eigenvectors (Maps)
Magnitude
Phase
normalized
0 phase
Eigenvalues
=1
Images

Example: ESPIRiT on Reduced FOV Imaging

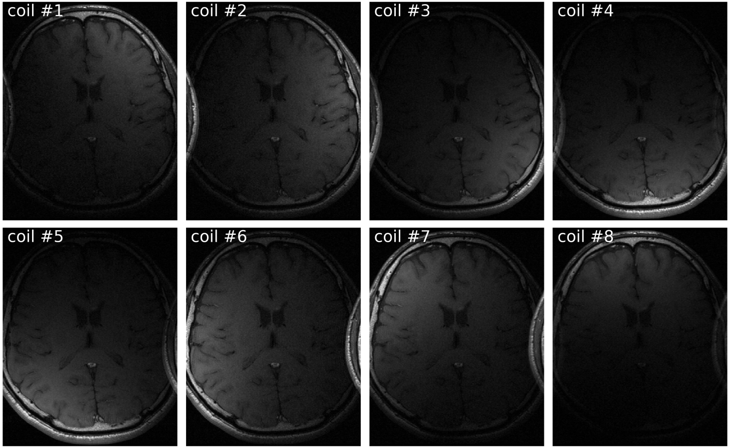

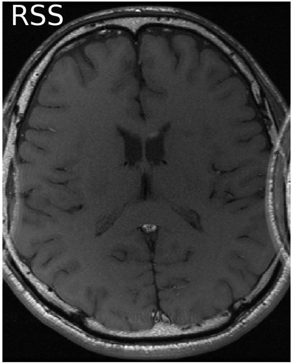

$$\text{RSS} : \sqrt{\sum_i (c_i \cdot \rho)^2}$$

Step #1: Retrospective Undersampling

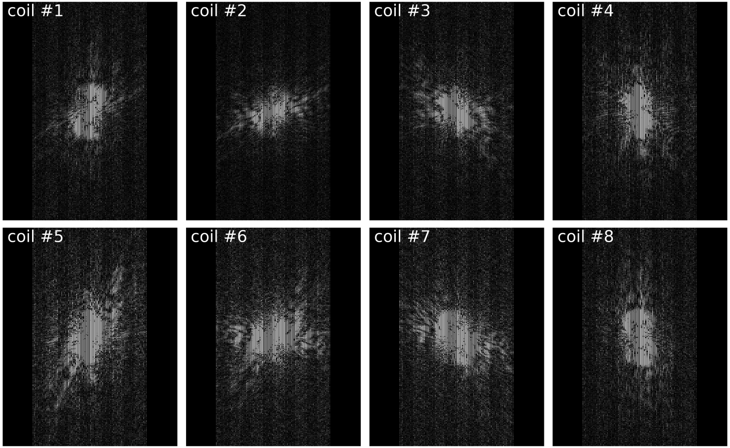

ZF (R=2)

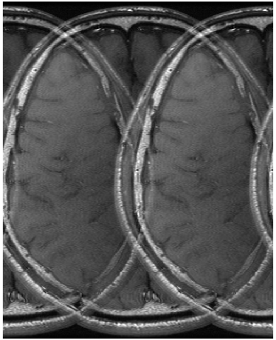

Curious about the black space on the left and the right sides of k-space?

→ Shimron E, Tamir JI, Wang K, Lustig M. Implicit data crimes: machine learning bias arising from misuue of public data. *Proc Natl Acad Sci U.S.A.* (2022).

Step #2: ESPIRiT with 1 Set of Coil Sensitivity Maps

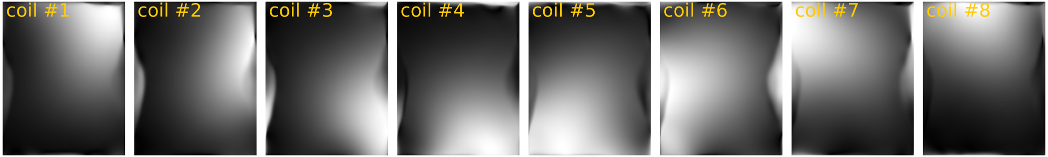

Step #3: SENSE Reconstruction

$$\underset{x}{\operatorname{argmin}} \|y - \mathbf{PFC}x\|_2 + \lambda \|x\|_2 \text{ with } x \in \mathbb{C}^{N_x \times N_y} \tag{18}$$

ZF (R=2)

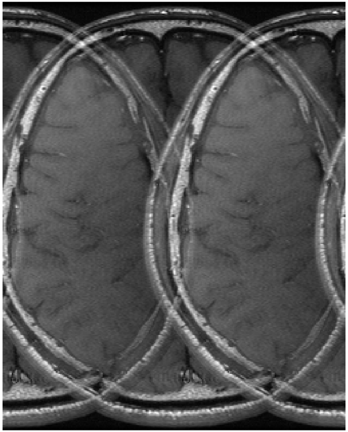

SENSE 1

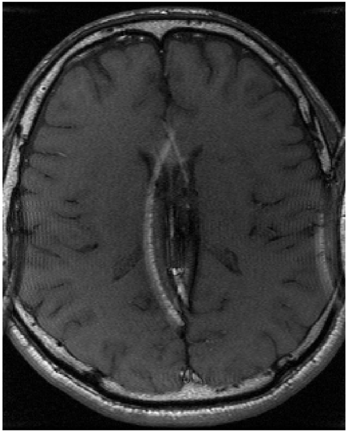

Step #4: ESPIRiT with 2 Sets of Coil Sensitivity Maps

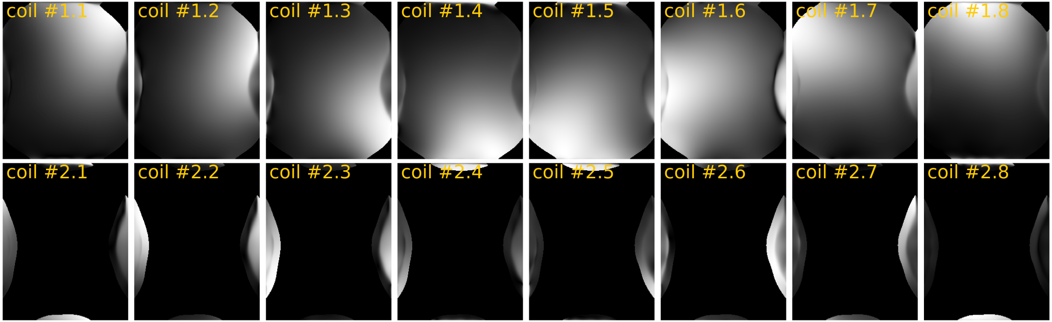

Step #5: Soft SENSE Reconstruction

$$\underset{x}{\operatorname{argmin}} \left\| y - \mathbf{PF} \sum_{j=1}^{2} (\mathbf{C}_j x_j) \right\|_2 + \lambda \|x\|_2 \text{ with } x \in \mathbb{C}^{N_x \times N_y \times 2} \quad (19)$$

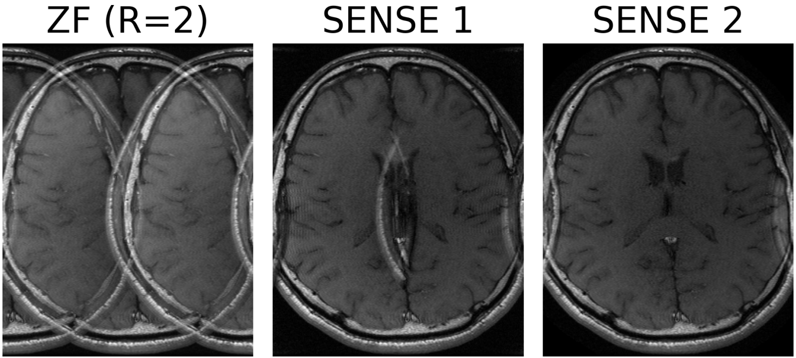

MUSSELS

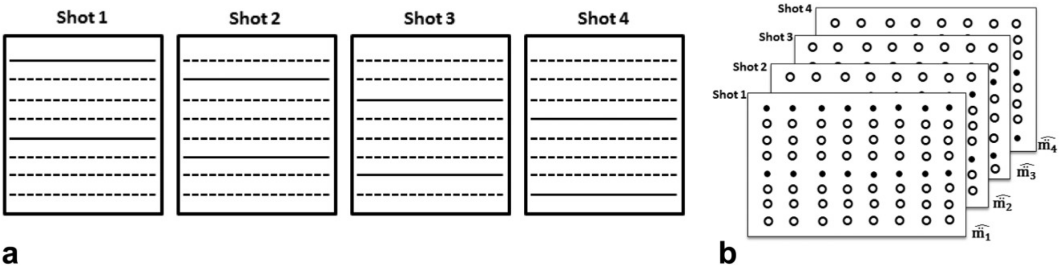
Shot 1
Shot 2
Shot 3
Shot 4
a
Shot 4
Shot 3
Shot 2
Shot 1
$\widehat{\ddot{m}}_4$
$\widehat{\ddot{m}}_3$
$\widehat{\ddot{m}}_2$
$\widehat{\ddot{m}}_1$
b

MUSSELS

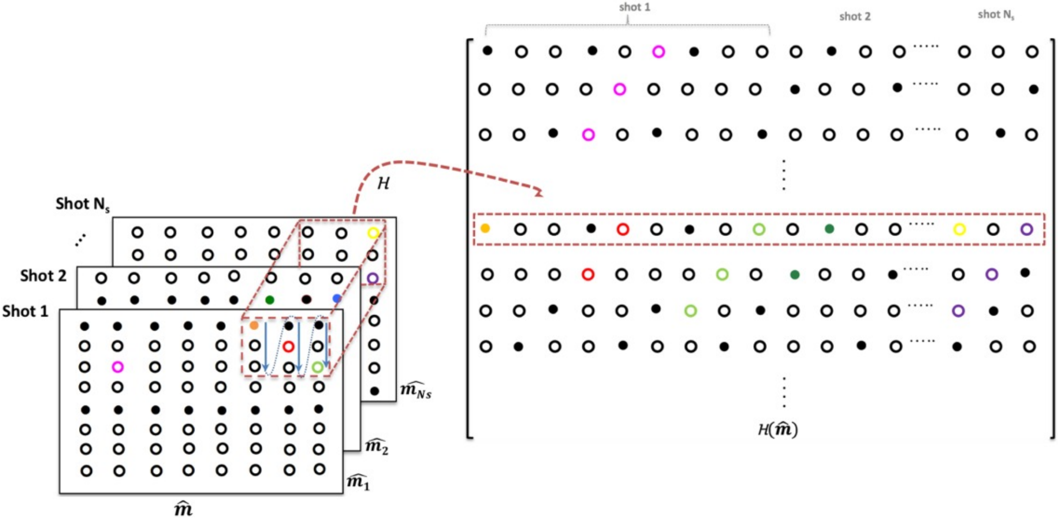

shot 1
shot 2
shot N_s
H
Shot N_s
Shot 2
Shot 1
$\hat{m}_{Ns}$
$\hat{m}_2$
$\hat{m}_1$
$\hat{m}$
$H(\hat{m})$

Comparing LLR and MUSSELS for Multi-Shot EPI [7]

8th DW image from 4-shot iEPI @ 1 mm ISO

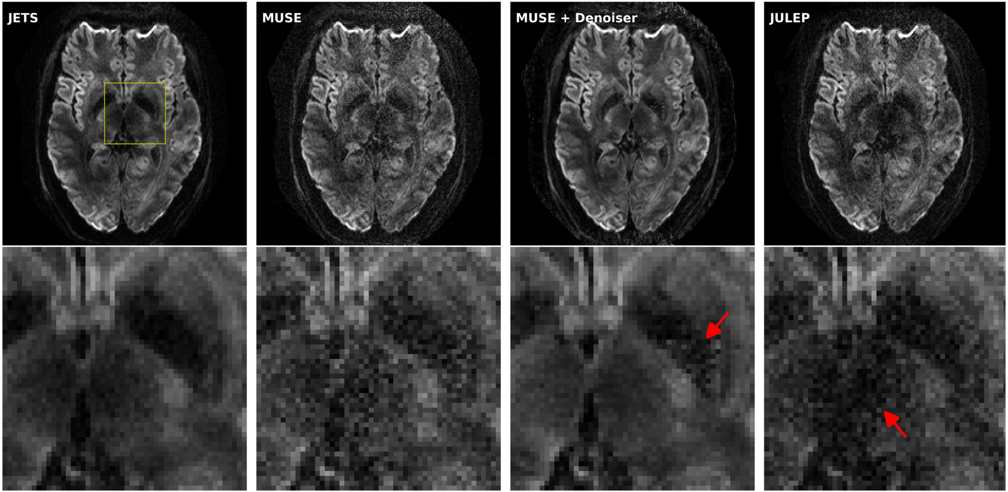

[7] https://doi.org/10.1162/imag_a_00085

Beyond Low Rank: 0.7 mm Isotropic Diffusion MRI

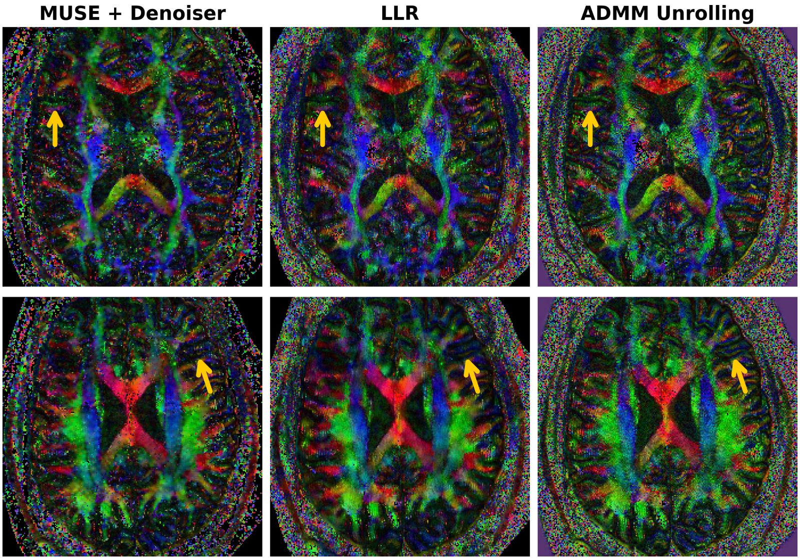

Questions

1. Why are images from Poisson sampling so blurry?

Questions

1. Why are images from Poisson sampling so blurry?

2. Given that MR images are complex-valued, how is soft thresholding performed?

Questions

1. Why are images from Poisson sampling so blurry?
2. Given that MR images are complex-valued, how is soft thresholding performed?
3. A dictionary is required to "learn" the subspace matrix Φ, what defines the shape of the dictionary?

Beyond Compressed Sensing: What do you spot in this figure?

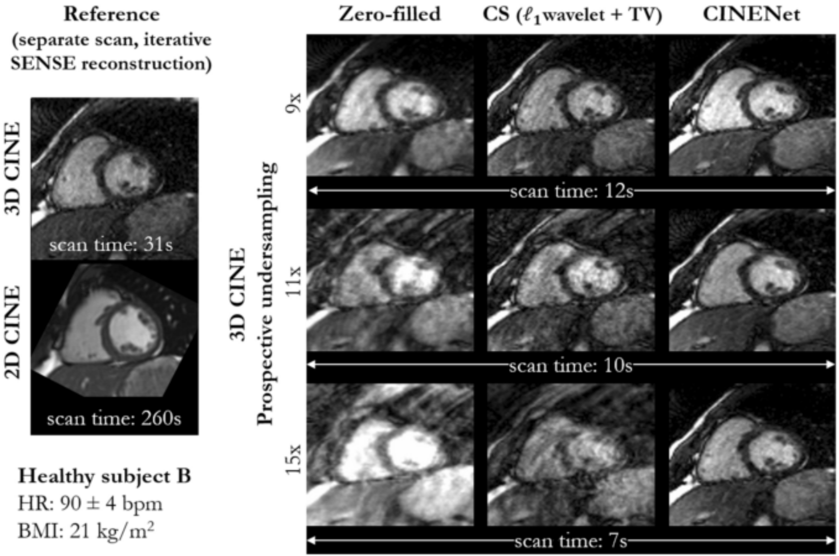

Summary

- Compressed sensing:
  1. incoherent sampling;
  2. sparsity $\ell 1$ constraint.

Summary

- Compressed sensing:
  1. incoherent sampling;
  2. sparsity $\ell 1$ constraint.
- Low rank:
  1. representation of high-dimensional data in low dimension;
  2. beneficial to multi-contrast, dynamic imaging.

Summary

- Compressed sensing:
  1. incoherent sampling;
  2. sparsity $\ell 1$ constraint.
- Low rank:
  1. representation of high-dimensional data in low dimension;
  2. beneficial to multi-contrast, dynamic imaging.
- If you are interested in the topics and look for research projects, reach out zgtan@umich.edu